

Self-assembly of neon into a quantum gel with crystalline structure in superfluid ^4He : Prediction from density functional theory

Jussi Eloranta*

Department of Chemistry and Biochemistry, California State University at Northridge, 18111 Nordhoff Street, Northridge, California 91330, USA

(Received 28 February 2008; published 2 April 2008)

Doping superfluid ^4He with a low concentration of neon atoms is predicted to lead to the self-assembly of “quantum gel” with crystalline structure, where each atom is isolated by a mixture of liquid and solid helium. The formation of this structure is shown to originate from the repulsive or attractive interactions between the solvent shells surrounding the neon atoms. The lattice geometry for neon atoms is predicted to be very sensitive to many-body effects, but by assuming a simple cubic symmetry, an upper limit estimate for neon atom density can be established (7% of bulk neon). Based on the energy estimates, this quantum gel structure is not related to the previously observed neon impurity helium solid. Experimental aspects of the quantum gel preparation are also briefly discussed.

DOI: [10.1103/PhysRevB.77.134301](https://doi.org/10.1103/PhysRevB.77.134301)

PACS number(s): 67.25.D-, 67.90.+z

I. INTRODUCTION

Superfluid ^4He is an exceptional solvent as it maintains a liquid phase down to 0 K temperature and exhibits remarkable quantum behavior below its lambda transition.¹ As such, it offers a unique environment to study liquid phase phenomena with minimal thermal perturbations. For example, the formation of impurity helium solids (IHSs) (consisting of N_2 , Ne, and D_2 , for example) in superfluid ^4He has been attributed to these special properties of the liquid.²⁻⁴ However, the exact mechanism of formation and structure of such solids is not well understood although recent progress has been made in this area.⁵ In addition to aggregation processes leading to the formation of these solids, the initial stage of chemical reactions may also be affected by the solvent and, thus, lead to unconventional reaction paths to be followed. Note that this scheme has been proposed in the literature but not confirmed by clear experimental observations.⁶ In conventional liquids, thermal perturbations tend to strongly diminish the effect of the solvent and, thus, interatomic and intermolecular forces dominate. In this paper, I consider the effect of the solvent in the aggregation of neon atoms at low temperatures and propose a new type of “quantum gel” that should exist in superfluid helium.

In the gas phase at low temperatures, the aggregation of neon atoms leads to the formation of solid neon due to the attractive van der Waals binding between the atoms. If the same process occurs in a low temperature liquid due to the diffusion of solvated neon atoms, the same van der Waals attraction is also expected to play a crucial role but, additionally, the liquid coordinate must be considered. After the first observation of N_2 IHS formation, it was suggested that a crust of solid helium surrounds the nitrogen clusters, forbidding their further aggregation and growth of solid N_2 .^{2,7,8} The solid layer around the clusters was thought to form because of the strong van der Waals attraction between the nitrogen cluster surface and helium. Despite many experimental studies on the subject, the microscopic level understanding of this phenomenon is severely lacking.²⁻⁴ For example, what is the exact role of the proposed solid helium layer and is this strong enough to overcome the cluster-

cluster interaction? To answer these questions, I will consider the diffusion mediated aggregation of Ne atoms solvated in superfluid helium as a prototypical system. First, the formation of a neon van der Waals dimer is modeled, and then the method is extended to describe the aggregation of spherical neon clusters in superfluid helium.

II. THEORY

To model a neon doped superfluid helium, three different interactions must be considered: (I) Ne-Ne, (II) Ne-liquid, and (III) liquid (i.e., liquid inhomogeneities). For (I), the *ab initio* Ne-Ne pair potential (V_{12}) is integrated over the zero-point nuclear wave functions for the two Ne atoms trapped in separate spherical solvation cavities (“bubbles”).⁹ Note that the standard Lennard-Jones potential models are not sufficiently accurate for the present calculations as they do not describe the dispersive tail of the pair potential correctly. In addition to pair interaction, there will be small many-body effects (e.g., shielding), which are ignored in the following calculations. Pair potential shielding by helium atoms located between the two neons is expected to reduce their binding and, therefore, result in a larger relative contribution of (II). The zero-point wave functions for Ne atoms trapped within solvation bubbles were obtained by a harmonic approximation, which resulted in a Gaussian function with about 2 Bohr full width at half maximum.¹⁰ Note that the zero-point motion along the Ne-Ne coordinate is not important here since the neon atoms are confined in “heavy” solvation bubbles. When considering the interaction between two neon clusters, the energy is obtained by integrating the *ab initio* pair potential over the neon densities in both clusters:

$$E = \iint \rho_{\text{Ne}_1}(r) V_{12}(|r - r'|) \rho_{\text{Ne}_2}(r') dr' dr, \quad (1)$$

where ρ_{Ne_i} denote the continuous neon atom densities in two identical clusters ($i=1$ and 2). The cluster densities are approximated by the following spherical form positioned at the center of cluster i :

$$\rho_{\text{Ne}_i}(r) = \rho_{0,\text{Ne}} \{1 - [1 + \alpha(R_0 - r)]e^{-\alpha(R_0 - r)}\}. \quad (2)$$

Here, $\rho_{0,\text{Ne}}$ corresponds to bulk neon density (6.591×10^{-3} a.u.), R_0 to the position of the interface, and α (2.4 a.u.; corresponding to about 2 a.u. interface thickness) is related to the barycenter of the cluster surface by $R_C \approx R_0 - 2/\alpha$. Note that this approximation treats the neon clusters as continuous objects and, hence, ignores all atomic level structures in them. For calculating (II), the *ab initio* He-Ne pair potential is employed.⁹ For both single Ne atom and Ne cluster, the interaction energy is obtained by integrating over the neon and helium densities in a similar fashion as was done in Eq. (1). The helium density appearing in this integral is determined by the density functional theory (DFT) model that is used for describing superfluid helium. The liquid contribution (III) is obtained by bosonic DFT, which is capable of describing strongly inhomogeneous superfluid ⁴He at 0 K.^{11,12} Note that this model has also been extended to non-zero temperatures but, for simplicity, we restrict this consideration to 0 K.¹³ Higher temperatures are expected to slightly widen the interfacial region between the neon impurities and superfluid helium. To accelerate the calculations and reduce the computer memory requirements, the solution of the resulting DFT equations is obtained in two-dimensional (2D) cylindrical coordinates by the imaginary time method, using the numerical procedures described in the Appendix. The liquid energy is obtained by evaluating the corresponding DFT energy functional for a converged liquid density (i.e., a four-dimensional integral in the present case). The total energy for the liquid containing the neon impurities is obtained as a sum of (I), (II), and (III) after performing a full imaginary time propagation for the liquid. By varying the distance R between the neon centers, the total energy can be calculated as a function of R . If the liquid follows the neon motion adiabatically, this defines a potential energy surface (PES) that governs their dynamics. In the gas phase, the PES would directly correspond to Ne-Ne van der Waals interaction, whereas in the liquid, the attraction or repulsion between the solvent layers surrounding the neon atoms will also contribute. Note that the total number of particles must be conserved in the calculations to ensure size consistency at different values of R .

III. RESULTS AND DISCUSSION

First, the formation of a neon van der Waals dimer in superfluid helium is modeled. The calculated PES is shown in Fig. 1 along with the gas phase Ne-Ne *ab initio* pair potential. When the two atoms approach, the solvent layers surrounding them begin to interact and this leads to a deviation from the gas phase potential. The liquid density along the Ne-Ne axis at two different distances is plotted in Fig. 2. The two liquid configurations shown correspond to a local maximum (“solvent layer maximum”) and a minimum (“solvent layer minimum”) on the PES, as indicated in Fig. 1. At the solvent layer minimum, there is a complete shell of helium surrounding the neon atoms (see also Fig. 3), whereas at the maximum, helium begins to retreat and pack on the sides (not shown). Finally, if the nuclei keep moving even

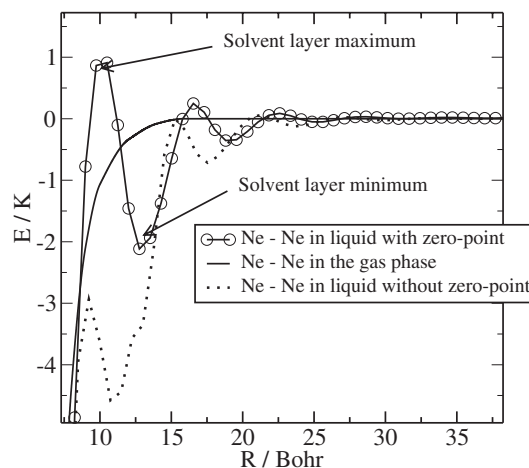


FIG. 1. Ne-Ne pair potentials in the gas phase (solid line) and in superfluid ⁴He (circles with zero point; dotted without zero point) as a function of atomic distance are shown.

closer to each other, helium is pushed out of the way completely and a Ne₂ van der Waals dimer forms. The attractive interaction in the solvent layer minimum arises from the van der Waals binding between the solvent shells, and the repulsion at the maximum from the Pauli exclusion between the closed shell helium atoms localized in the solvent shells. The overall effect of the solvent layer repulsion and attraction is to introduce an energy barrier for Ne₂ formation, which is about 3.2 K (in units of kT). The effect of the neon atom zero-point motion within the solvation bubble is also demonstrated in Fig. 1. Interestingly, without the zero-point motion for neon atoms, the energy barrier in the PES becomes smaller because the effective Ne-Ne potential is stronger and the solvation bubble for the neon atoms is smaller. Overall, the main features of the PES still remain the same. If the liquid temperature is well below the solvent induced barrier height (in Kelvin), dimerization of neon atoms becomes forbidden. If the temperature is of the same order as the energy barrier, this structure is expected to be only metastable. A

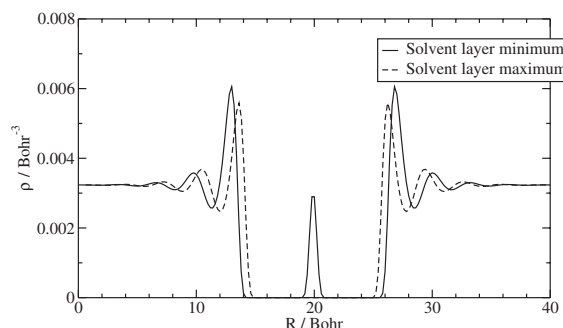


FIG. 2. Cuts along the Ne-Ne coordinate showing the superfluid ⁴He density at two different values of R . The solid line corresponds to $R=12.8$ Bohr and the dashed line to $R=10.5$ Bohr. See Fig. 1 for the locations of these positions on the PES (i.e., solvent layer minimum and solvent layer maximum, respectively). The densities correspond to results from DFT calculations with the nuclear zero-point correction included for neon.

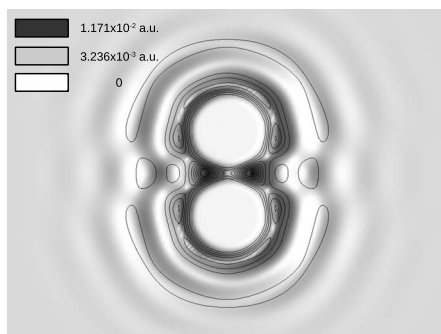


FIG. 3. 2D contour plot of superfluid helium density at the solvent layer minimum geometry for Ne-Ne. Note that a ring of solid helium exists around the neck of the molecular axis. The data shown in Fig. 2 correspond to a one-dimensional cut along the axis.

simple Arrhenius based estimate predicts that a liquid temperature around 100 mK is required to stabilize Ne_2 at the solvent layer minimum for a period of 1 s. It should be noted that this estimate strongly depends on the solvent induced barrier height and is therefore rather sensitive to the pair potentials used. For example, the application of Lennard-Jones potentials leads to considerably higher solvent barrier heights (about 7 K corresponding to 300 mK temperature). Given that the nuclear dynamics is sufficiently slow, the surrounding liquid is expected to respond adiabatically and the PES shown in Fig. 1 is valid. In the case of a nonadiabatic response, however, an even higher effective solvent layer barrier is expected to arise from the unrelaxed solvent layers and, thus, the PES in Fig. 1 yields a lower limit for the solvent layer barrier. Since Ne atoms have a relatively small mass, it is necessary to consider quantum mechanical tunneling, which could effectively overcome the barrier and lead to the formation of a Ne_2 dimer. However, a neon atom in a solvation bubble is a heavy object in the liquid because its effective mass depends on the size of the bubble and the mass of the solvent layer surrounding the atom. For this reason, tunneling is not expected to be very effective because it would involve large rearrangements in the liquid.

Based on the effective pair potential shown in Fig. 1, superfluid helium doped with a low concentration of neon atoms should self-assemble into a quantum gel with a crystalline order, where each neon atom is surrounded by a dense layer of helium. It is not clear *a priori* what kind of lattice geometry should form, in particular, because many-body effects (including those associated with interactions of solvent layers between multiple atoms) remain unaccounted for. Some simple models can be considered by inspecting the liquid density at the solvent layer minimum (see Fig. 3). Within a cubic symmetry, both body-centered and face-centered structures are expected to be unstable because of the strong overlap between the high density helium belt around Ne-Ne and the solvent layers of other neon atoms. For this reason, a simple cubic symmetry should be more favorable. Note that this is not certainly the only possibility but, in order to obtain the exact crystal symmetry, additional calculations are required in three dimension. If a simple cubic symmetry is assumed and the nearest neighbor distance is about 12.7 Bohr, the atomic neon density should be 4.9

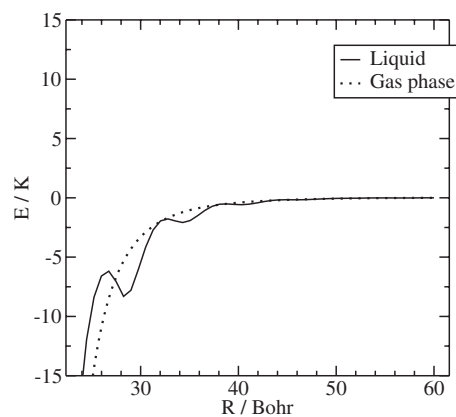


FIG. 4. The effective pair potential between spherical Ne_{22} - Ne_{22} clusters ($R_C \approx 9.2$ Bohr; solid line) and the corresponding gas phase potential (dotted line) are shown. The distance is measured between the centers of the clusters.

$\times 10^{-4}$ a.u. (7% of bulk neon) or less since the Ne-Ne distance is expected to be stretched by the many-body interactions. The other plausible crystal geometries tend to lead to slightly sparser structures and to lower neon atom densities. Hence, only an upper limit estimate for neon atom density can be obtained. It should be noted that this density estimate for a neon quantum gel is considerably higher than has been observed for neon IHS (about 1% of bulk neon). It is possible that the crystalline structure in the quantum gel has “defects,” where a neon atom (or atoms) is missing from the lattice, but this should not significantly contribute to the density estimate. Because many-body interactions are expected to increase the solvent layer energy barrier for the formation of solid neon, the gel structure should considerably be more stable than predicted by the pair potential in Fig. 1. Thus, a metastable seed (i.e., Ne-Ne at the solvent layer minimum) may lead to its growth even at higher temperatures. For melting to occur, superfluid helium must be squeezed out of the neon portion completely. Note that to experimentally prepare this type of quantum gel, one has to use a very dilute Ne/He gas mixture, which should be deposited on a superfluid helium surface at ≤ 100 mK temperature. The basic idea of the experiment has been described earlier.^{2,4,5,7,8} To avoid clustering in the gas phase, a high-velocity Ne/He gas jet should be used for sample deposition. Note that much higher temperatures (≥ 1.5 K) have been used in the previous experiments, which have focused on IHS formation.

If the clustering occurs already before entering the liquid phase, a further aggregation of the clusters in the liquid might also be affected by the solvent layers. To demonstrate this behavior, a neon cluster with $R_C \approx 9.2$ a.u. (approximately 22 atoms) was chosen. The resulting PES for two such clusters approaching each other is shown in Fig. 4. Clearly, the solvent layer interaction is present but the long-range cluster-cluster binding appears to dominate. From the nuclear dynamics point of view, this long-range cluster-cluster binding gives probably enough excess energy for the clusters to overcome the solvent layer energy barrier. It should be noted, however, that such dynamics would necessarily also involve a dissipation of energy via sound emission

and, therefore, not all the excess energy would be available for crossing the barrier. Thus, a quantum gel-like structure is not expected to form from neon clusters, which have formed in the gas phase or on the liquid surface.

Significant clustering in the gas phase and on the superfluid helium surface has been observed during the deposition phase of N₂ IHS samples.⁴ In neon IHS samples, such clustering should contribute to the growth of a highly porous solid filled with superfluid helium. This expectation is in agreement with the model recently suggested by Kiryukhin *et al.*⁵ Furthermore, similar porous solids containing superfluid helium have also been formed from alkali metal atoms, which have essentially repulsive interaction with helium and no strongly bound solvent layer structure.¹⁴ In contrast, the neon quantum gel described above has high crystalline order and is held together by bound solvent layers. Furthermore, neon IHS samples have been previously prepared at relatively high temperatures (≥ 1.5 K), where the neon quantum gel is predicted to be unstable. Therefore, it can be concluded that the neon quantum gel structure does not correspond to neon IHS and appears not to have been observed experimentally yet.

ACKNOWLEDGMENT

The Research Corporation (Tucson, Arizona) is thanked for financial support.

APPENDIX

The energy functional for superfluid ⁴He at 0 K is expressed as^{11,12}

$$E[\psi(r,t)] = \frac{\hbar^2}{2M_{\text{He}}} \int |\nabla\psi(r,t)|^2 dr + \frac{1}{2} \int \int \rho(r,t) U_l^e(|r-r'|) \times \rho(r',t) dr' dr + \frac{c_2}{2} \int \rho(r,t) [\bar{\rho}(r,t)]^2 dr + C \int \rho(r,t) (1 + \tanh\{\beta[\rho(r,t) - \rho_m]\}) dr + \frac{c_3}{3} \int \rho(r,t) [\bar{\rho}(r,t)]^3 dr, \quad (\text{A1})$$

where the liquid density at point r is given by $\rho(r,t) = |\psi(r,t)|^2$, M_{He} is the helium atom mass, $\bar{\rho}$ denotes a spherical average of the liquid density ρ over a fixed radius $h = 2.1903 \text{ \AA}$, $c_2 = 2.411 857 \times 10^4 \text{ K \AA}^6$, $c_3 = 1.858 496 \times 10^6 \text{ K \AA}^9$, $C = 0.1$ hartree, $\beta = 40 \text{ \AA}^3$, and $\rho_m = 0.37 \text{ \AA}^{-3}$. The screened He-He Lennard-Jones interaction U_l^e is given by ($\sigma = 2.556 \text{ \AA}$ and $\epsilon = 10.22 \text{ K}$)

$$U_l^e(r) = \begin{cases} 4\epsilon \left[\left(\frac{\sigma}{r}\right)^{12} - \left(\frac{\sigma}{r}\right)^6 \right] & \text{when } r \geq h \\ 0 & \text{when } r < h. \end{cases} \quad (\text{A2})$$

The corresponding functional derivative is^{12,15}

$$\frac{\delta E}{\delta \psi^*(r,t)} = -\frac{\hbar^2}{2M_{\text{He}}} \Delta\psi(r,t) + \int \rho(r',t) U_l^e(|r-r'|) dr' \psi(r,t) + \left[\frac{c_2}{2} [\bar{\rho}(r,t)]^2 + c_2 \int \Pi_h(|r-r'|) \rho(r',t) \bar{\rho}(r',t) dr' \right] \psi(r,t) + \left[\frac{c_3}{3} [\bar{\rho}(r,t)]^3 + c_3 \int \Pi_h(|r-r'|) \rho(r',t) [\bar{\rho}(r',t)]^2 dr' \right] \psi(r,t) + C [1 + \tanh\{\beta[\rho(r,t) - \rho_m]\}] \psi(r,t) + \beta \rho(r,t) (1 - \tanh^2\{\beta[\rho(r,t) - \rho_m]\}) \psi(r,t), \quad (\text{A3})$$

with a spherical averaging function denoted as

$$\Pi_h(x) = \begin{cases} \frac{3}{4\pi h^3} & \text{when } x \leq h \\ 0 & \text{elsewhere.} \end{cases}$$

The angular part in the Lennard-Jones term can be integrated analytically as follows:

$$\int \rho(r') U_l^e(|r-r'|) dr = 8\epsilon \int_{r'=0}^{\infty} \int_{z'=-\infty}^{\infty} \rho(r',z') r' \left[\sigma^{12} \int_C^{\pi} \Omega_1(a,b) - \sigma^6 \int_C^{\pi} \Omega_2(a,b) \right] dz' dr' \quad (\text{A4})$$

with

$$C = \arccos \left[\max \left(-1, \min \left(1, \frac{h^2 - a}{b} \right) \right) \right], \\ a = r^2 + r'^2 + (z - z')^2, \quad b = -2rr',$$

where C has a value between 0 and π . The auxiliary functions Ω_1 and Ω_2 are

$$\int \Omega_1(a,b) = \int \frac{dx}{[a+b \cos(x)]^6} = \frac{1}{120a^6} \times \left[\frac{30(15\gamma^4 + 40\gamma^2 + 8) \arctan\left(\frac{(1-\gamma)\tan(x/2)}{\sqrt{1-\gamma^2}}\right)}{(1-\gamma^2)^{11/2}} - \frac{\gamma \sin(x)}{(1-\gamma^2)^5 [1+\gamma \cos(x)]^5} \right. \\ \left. \times \{24(1-\gamma^2)^4 + 54(1-\gamma^2)^3 [1+\gamma \cos(x)] + 2(1-\gamma^2)^2 (16\gamma^2 + 47) [1+\gamma \cos(x)]^2 \right. \\ \left. + 7(22 + \gamma^2 - 23\gamma^4) [1+\gamma \cos(x)]^3 + (64\gamma^4 + 607\gamma^2 + 274) [1+\gamma \cos(x)]^4 \}, \right] \quad (\text{A5})$$

$$\int \Omega_2(a,b) = \int \frac{dx}{[a+b \cos(x)]^3} = \frac{1}{a^3} \left[\frac{(2+\gamma^2) \arctan\left(\frac{(1-\gamma)\tan(x/2)}{\sqrt{1-\gamma^2}}\right)}{(1-\gamma^2)^{5/2}} + \frac{\gamma \sin(x) [\gamma^2 - 3\gamma \cos(x) - 4]}{2(\gamma^2 - 1)^2 [1+\gamma \cos(x)]^2} \right], \quad (\text{A6})$$

where $\gamma=b/a$. The short-range correlation terms are given by

$$\frac{c_n}{n} [\bar{\rho}(r)]^n + c_n \int \Pi_h(|r-r'|) \rho(r') \bar{\rho}(r)^n dr' = \frac{c_n}{n} [\bar{\rho}(r,z)]^n + c_n \int_{r'=0}^{\infty} \int_{z'=-\infty}^{\infty} \Pi'_h(a,b) \rho(r',z') [\bar{\rho}(r',z')]^{n-1} r' dz' dr', \quad (\text{A7})$$

where

$$\bar{\rho}(r,z) = \int_{r'=0}^{\infty} \int_{z'=-\infty}^{\infty} \rho(r',z') \Pi'_h(a,b) r' dz' dr'$$

and

$$\Pi'_h(a,b) = \frac{6}{4\pi h^3} \arccos \left[\max \left(-1, \min \left(1, \frac{h^2 - a}{b} \right) \right) \right].$$

The details for the time propagation of the DFT equations are given elsewhere.¹⁵

*jussi.eloranta@csun.edu

¹J. Wilks, *The Properties of Liquid and Solid Helium* (Clarendon, Oxford, 1967).
²E. B. Gordon, L. P. Mezhov-Deglin, and O. F. Pugachev, *JETP Lett.* **19**, 63 (1974).
³V. V. Khmelenko, S. I. Kiselev, D. M. Lee, and C. Y. Lee, *Phys. Scr.* **102**, 118 (2002).
⁴E. A. Popov, J. Eloranta, J. Ahokas, and H. Kunttu, *Low Temp. Phys.* **29**, 510 (2003).
⁵V. Kiryukhin, E. P. Bernard, V. V. Khmelenko, R. E. Boltnev, N. V. Krainyukova, and D. M. Lee, *Phys. Rev. Lett.* **98**, 195506 (2007).
⁶E. Lugovoj, J. P. Toennies, and A. Vilesov, *J. Chem. Phys.* **112**, 8217 (2000).
⁷E. B. Gordon, V. V. Khmelenko, A. A. Pelmenev, E. A. Popov, and O. F. Pugachev, *Chem. Phys. Lett.* **155**, 301 (1989).

⁸E. B. Gordon, V. V. Khmelenko, A. A. Pelmenev, E. A. Popov, and O. F. Pugachev, *Chem. Phys.* **170**, 411 (1993).
⁹S. M. Cybulski and R. R. Toczylowski, *J. Chem. Phys.* **111**, 10520 (1999).
¹⁰J. Eloranta and V. A. Apkarian, *J. Chem. Phys.* **116**, 4039 (2002).
¹¹F. Dalfovo, A. Latri, L. Pricapenko, S. Stringari, and J. Treiner, *Phys. Rev. B* **52**, 1193 (1995).
¹²F. Ancilotto, M. Barranco, F. Caupin, R. Mayol, and M. Pi, *Phys. Rev. B* **72**, 214522 (2005).
¹³F. Ancilotto, F. Faccin, and F. Toigo, *Phys. Rev. B* **62**, 17035 (2000).
¹⁴P. Moroshkin, A. Hofer, S. Ulzega, and A. Weis, *Nat. Phys.* **3**, 786 (2007).
¹⁵L. Lehtovaara, T. Kiljunen, and J. Eloranta, *J. Comput. Phys.* **194**, 78 (2004).